

Tribological performance of hybrid filtered arc-magnetron coatings. Part II: Tribological properties characterization

Vladimir Gorokhovskiy^{a,*}, Chris Bowman^a, Paul Gannon^a, Dave VanVorous^a,
Andrey A. Voevodin^b, A. Rutkowski^b

^a *Arcomac Surface Engineering, LLC, Bozeman, Montana 59715, USA*

^b *AFRL/MLBT Wright Patterson AFB, Ohio, USA*

Received 13 June 2006; accepted in revised form 16 November 2006

Available online 26 December 2006

Abstract

Nano-structured coating architectures were developed to provide a best blend of corrosion and wear resistance for high chromium content steels used in aerospace bearing and gear applications. A hybrid filtered arc-magnetron deposition process was employed to deposit functionally graded, multilayered and nanocomposite TiCrN/TiCrCN+TiBC cermet coatings on carburized steel substrates. Coatings exhibited excellent adhesion to the carburized surfaces and had hardness in the range of 23–25 GPa. Tribological properties of the coatings were characterized by: pin-on-disk COF, lubricated sliding, reciprocating sliding, and 3 ball half thrust bearing tests in dry and lubricated environments at high contact stresses. Both polyester and perfluoropolyalkylethers (PFPAE) based lubricants were used to evaluate coating performance with neutral and chemically aggressive lubrication. Sliding friction and reciprocating sliding wear tests were performed using modified disk-on-ring and point-on-disk arrangements, respectively. Contact stresses were estimated using the Hertzian contact formula (sliding friction), and through direct measurements of contact areas by SEM (reciprocating sliding). Low-speed thrust bearing high load rolling contact was evaluated at 350 °C, using Si₃N₄ balls and PFPAE-based lubricant, at contact stresses of ~3.2 GPa. Aggressive corrosion testing was performed on coated samples using MIL-STD-810F “salt-fog” testing. Wear and corrosion behavior was investigated using SEM/EDS, EDX, AFM, profilometry, and optical microscopy. The influence of coating architecture on wear properties was investigated. Multifold improvements in the surface dry and lubricated wear life, reduction of the dry friction coefficient, prevention of corrosion attack from the products of PFPAE lubricant degradation, and improvement of salt-fog corrosion resistance are demonstrated.

© 2006 Elsevier B.V. All rights reserved.

Keywords: Filtered-arc; Nanocomposite; PFPAE; Corrosion

1. Introduction

Multilayered nano-structured films with elaborate compositions of metal and ceramic material have been reported for wear, corrosion and erosion protective coatings as well as for tribological applications. The production of such multi-component and multiphase coatings is a logical development of the multiple-layer concept, which states that individual layers within a coating system can be effectively engineered to address the specific, and often opposing, design requirements of a component or component system to be coated. The present studies, (parts I and II), surround the development (part I) and testing (part II) of a

functionally graded nano-structured multiple-layer coating architecture consisting of two segments separated by an intermediate zone, similar to the coatings discussed in [1–7]. Design principles for this graded multilayer concept were initially suggested for heavily loaded tribological pairs by Voevodin et al. in [8,9]. These principles are further developed here to address the high temperature, high load, and corrosion resistance requirements originating from advanced aerospace bearings and gears applications, leading to the development of an original TiCrN/TiCrCN+TiBC multilayer coating system.

Carburized Pyrowear 675, an alloy that has shown promise in advanced bearing and gear applications as compared to more commonly used alloys such as 440C, M50, and M50-Ni1, was selected as the primary coating substrate [10,11]. Pyrowear samples were coated with a two segment coating system

* Corresponding author. Tel.: +1 406 522 7620; fax: +1 406 522 7617.

E-mail address: vigase@aol.com (V. Gorokhovskiy).

consisting of a bottom TiCr/TiCrN multilayer corrosion resistant segment, a TiCrCN gradient intermediate zone, and a TiBC single layer (SL), or a TiBC/BC multilayer (ML) top wear resistant segment. The bottom segment TiCr/TiCrN multilayer + TiCrCN gradient (referred to as the TiCrN/TiCrCN segment) nanostructures both ceramic and metallic layers providing a super-lattice with a bi-layer period at a nanometer scale; a concept that is widely employed for corrosion resistant applications [2,3,6,12–14]. Although primarily intended for corrosion resistance the bottom segment architecture also provides good adhesion, toughness, and beneficial compressive stresses to the substrate surface [2,5–7,14–16]. The intermediate zone, separating the bottom and top coating segments, consists of a graded composition providing smooth transition from the nitride based bottom coating segment to the carbide based top coating segment. This structure is tailored for optimal compatibility and stress management of the adjacent layers. The intermediate zone enhances the bond/adhesion of the top (low friction, wear resistant) coating segment to the bottom (corrosion resistant) coating segment. The coating system top segment is designed to address the low friction and wear resistance requirements of advanced contact applications. TiBC (SL) and TiBC/BC (ML) top segment configurations are low friction coatings capable of operating in dry friction conditions as solid lubricant material [5,14,16,17]. Adding boron carbide to the multi-phase tribological coatings can improve corrosion resistance and thermal-chemical compatibility with lubricants at elevated temperatures, in addition boron carbide is recommended for wear applications operating under high friction loads, such as cutting and forming tools [5,7,14,18–20].

This paper reports on the friction, wear, and corrosion behaviors of the multi-segment TiCrN/TiCrCN+TiBC coating system applied to carburized Pyrowear 675 substrates and also compares testing results for uncoated carburized Pyrowear 675 tested under the same conditions. Contact pairs representative of bearing and gear applications were characterized in the following areas: dry sliding friction coefficient, lubricated sliding, dry/lubricated reciprocating sliding, high temp/high load rolling contact PFPPE lubricant compatibility, and salt fog corrosion resistance.

2. Experimental details

A detailed description of Filtered Arc Plasma Source Ion Deposition (FAPSID) technology and the hybrid Large Area Filtered Arc Deposition-Unbalanced Magnetron (LAFAD-

UBM) process as well as the coating sample matrix used in this work are presented in Part I of this paper [21]. In addition to general coating properties characterization presented in [21] the following test methodologies were used for further evaluation of tribological, wear, and corrosion resistance properties. Of the coatings produced in [21] two primary coating candidates shown in Table 1 were selected for evaluation in this effort for advanced aircraft bearings and gears applications. For simplicity the TiBC/BC multilayer top segment variation is referred to as the TiBC ML segment. For coated/coated contact regimes one counterpart was coated with a primary architecture, either TiCrN/TiCrCN+TiBC (SL or ML), and the opposing counterpart was coated with a TiCrN/TiCrCN 2 μm bottom segment only. For corrosion testing TiCrN/TiCrCN segment thickness was used as a comparative variable, in this case TiCrN/TiCrCN coatings at 1.2 μm thickness are also compared.

2.1. Coating coefficient of friction

Dry friction and wear tests were performed at Wright-Patterson Air Force Base Air Force Research Lab using a pin-on-disc tribometer inside an airtight chamber. Tests were conducted on coated carburized Pyrowear 675 discs under atmospheric pressure in moist air with $40 \pm 1\%$ relative humidity at 25 °C. For pin materials, 6.35 mm in diameter M50 steel and Si_3N_4 balls were used. A load of 100 g and rotational speed of 200 rpm were used in all experiments, with sliding speeds of about 200 mm/s. One disk revolution corresponded to about 50 mm of sliding distance. Friction coefficients were recorded for 10^4 sliding cycles (\sim sliding distance of 500 m), which was sufficient to achieve a steady state friction coefficient.

2.2. Lubricated sliding wear

A turbine oil lubricated disc-on-ring test was performed using a modified Timken rig developed at Arcotec Surface Engineering. The test was characterized as sliding “disc-on-ring” line contact. Coated carburized Pyrowear 675 discs were tested against both coated (2 μm thick TiCrN/TiCrCN) and uncoated Timken (A4138) tapered roller bearing outer rings. The rotating ring was partially submerged in 30 mL of Aeroshell Turbine Oil 555 (DOD-85734 (AS)) at 25 °C. Initial testing was conducted for a 1.4 GPa contact stress to model stresses predicted for advanced gear applications, but nearly instantaneous severe mechanical failure of uncoated samples did not allow a good comparison with coated samples. Instead a 90 N load was applied during testing to produce a 200 MPa contact stress calculated by the Hertzian stress formula for elastic line contact [22]. Testing was conducted at 260 rpm, for a period of 2 min, resulting in an approximate sliding distance of 58 m. Wear scars were analyzed qualitatively by optical microscopy and SEM. Analytical results for oil particulate count were obtained by Induction Coupled Plasma Mass Spectroscopy (ICP-MS).

2.3. Lubricated/dry reciprocating sliding wear

A reciprocating sliding point-on disk test was developed for characterization of reciprocating sliding wear resistance at high

Table 1
Pyrowear 675 coating matrix for tribological evaluation

Test sample	Coating
Pyrowear 675 — 1" dia \times 0.3125" coupon	n/a (uncoated baseline)
Pyrowear 675 — 1" dia \times 0.3125" coupon	TiCrN/TiCrCN 2 μm + TiBC SL 1 μm
Pyrowear 675 — 1" dia \times 0.3125" coupon	TiCrN/TiCrCN 2 μm + TiBC ML 1 μm
Timken A4138 ring or 440C dental scaler (coated test counterparts)	TiCrN/TiCrCN 2 μm

pointed loads, Fig. 1a. This test employed a coated (TiCrN/TiCrCN) dental scaler tip with a sharpened edge to slide in a reciprocative manner (0.8 mm sliding distance) against coated and uncoated carburized Pyrowear 675 coupons. Scalers used for coating were 440C stainless steel of hardness 58 HRC. Lubricated sliding conditions using Aeroshell Turbine Oil 555 (DOD-85734) at 25 °C and dry sliding conditions at 25 °C were investigated, humidity was not actively controlled (~35% RH). To accelerate the damage produced in testing, a load of 300 g was applied at the point of contact. Due to the shape of the scalers used in testing the contact was classified as maturing pointed to linear contact. As a result, minimum contact stresses were estimated by dividing the applied load by the measured wear area produced on the scaler edge at the end of testing (measured by SEM Fig. 1b). At the onset of testing initial high pointed contact stresses >1.4 GPa (>200 ksi) were estimated to mature to 200 MPa (30 ksi) by the completion of testing. All tests were conducted for 10,000 strokes, stroke amplitude of ~800 μm, and a rate of 4 Hz. The damaged surface regions of both the test coupon and scaler were investigated using reflective optical microscopy, SEM/EDS and contact profilometry.

2.4. High load rolling contact/high temperature PFAPE lubricant compatibility

Evaluation of high temperature PFAPE corrosion under high load rolling conditions was conducted using a thrust bearing ball-

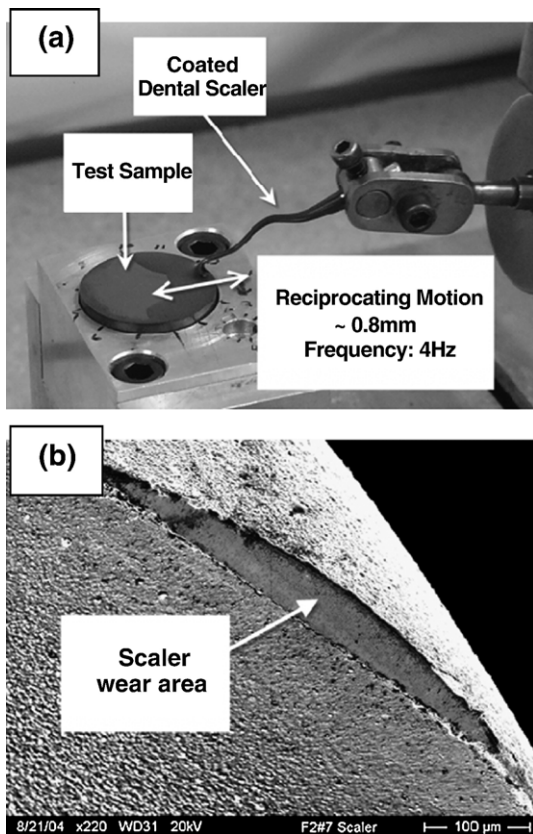


Fig. 1. (a) Image of reciprocating sliding test rig which uses sharp coated dental scalers as the indenter. (b) SEM image of a 2.0 μm TiCrN/TiCrCN coated scaler after 10,000 cycles reciprocating sliding test, wear area is calculated and used to approximate the contact stress from a known loading.

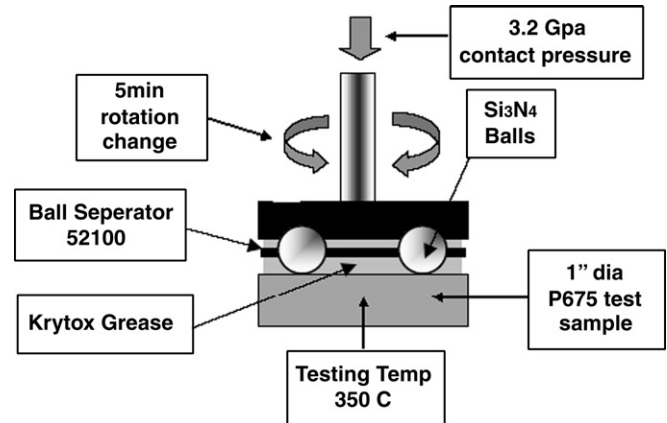


Fig. 2. Schematic of thrust bearing ball-on-disk test fixture used for evaluation of high temperature PFAPE lubricant compatibility testing.

on-disk test fixture shown in Fig. 2. The test allowed for the simulation of rolling contact at 350 °C under a 3.2 GPa Hertzian stress in the presence of PFAPE-based lubricant. The testing rig was designed to allow for adjustment in sample loading, rotation speed, and timed rotation direction changes. Contact stresses were evaluated by the standard Hertz equation, with the assumption of sphere on plane contact [22]. Actual loadings were measured and averaged over 25 instances, for actual testing conditions of 3.24 GPa ± 0.03 GPa. Three (3 mm) Si₃N₄ ball bearings (Boca) were arranged 120° from each other in an ~12 mm ID race (Boca), coated with Krytox XHT-BDX lubricant, and tested in rolling contact against coated and uncoated carburized Pyrowear 675 disk coupons at 350 °C. Rolling speed was approximately 2 rpm with a 5 min period between rotation direction changes. Testing was conducted for 2 h, 24 h, and 200 h time frames. Wear tracks produced in rolling contact fatigue (RCF) testing were analyzed by reflective optical microscopy, SEM and contact profilometry. The corrosion byproducts were analyzed by EDX.

2.5. Corrosion testing

Corrosion resistance testing of coated and uncoated carburized Pyrowear 675 was performed at Garwood Laboratories Inc. of Pico River, CA according to a neutral salt fog MIL-STD-810F designation similar to ASTM B117 [23]. All samples were batch tested at the following parameters, 35 °C, 5% NaCl solution, pressure 1atm, and duration 48 h. Testing results were analyzed visually and by optical microscopy.

3. Results and discussion

3.1. COF testing results

A summary of COF results for the tested friction pairs is shown in Table 2. The results show that multi-layered nano-composite coatings with carbide containing upper segments are effective in reducing dry sliding friction for materials commonly used in advanced bearing and gear applications. All coated coupons demonstrated time dependent friction behavior; representative examples are shown in Figs. 3(a), (b), 4(a) and (b) for TiBC SL

Table 2
Pin-on-disk COF results for uncoated and coated friction pairs

Steady state COF results for selected materials		
Rotating disk material	Stationary pin material	
	440C (COF)	Si ₃ N ₄ (COF)
Uncoated Pyrowear 675 (carbuzized)	0.5 +/- 0.2	0.75 +/- 0.5
TiCrN/TiCrCN (2 μm) + TiBC SL (1 μm)	0.35 +/- 0.05	0.38 +/- 0.02
TiCrN/TiCrCN (2 μm) + TiBC ML (1 μm)	0.45 +/- 0.1	0.4 +/- 0.03

and TiBC ML test runs. Maximum friction values were recorded in contact with 440C and Si₃N₄ for TiBC ML upper segments after ~250 cycles, while the initial friction slope for TiBC SL upper segments was less steep resulting in maximum friction values at ~1000 cycles. This could indicate that the initial wear process for TiBC SL coatings is less aggressive than for TiBC ML coatings, this indication is further supported by the average

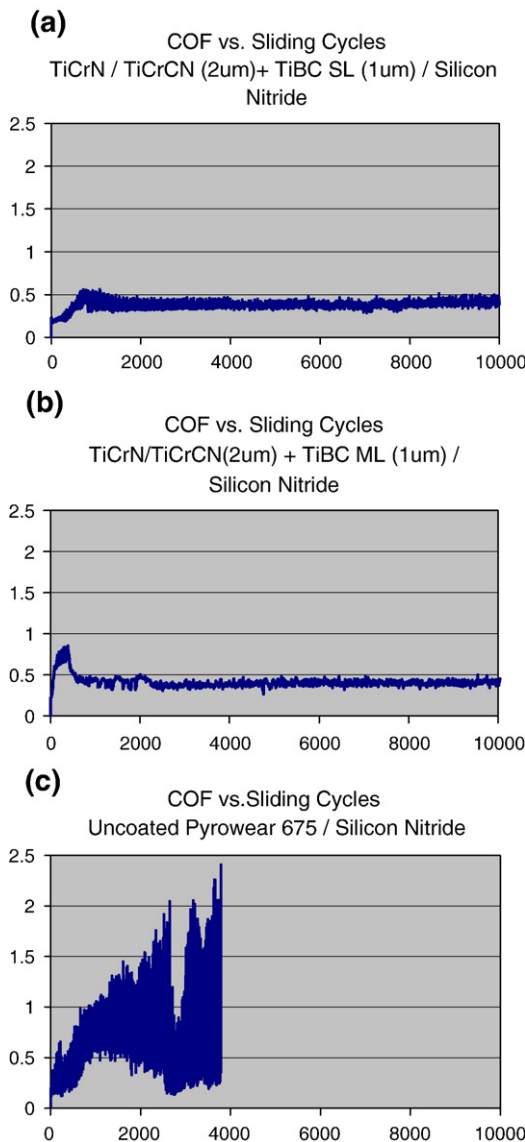


Fig. 3. Time dependant friction behavior of TiCrN–TiCrCN+TiBC SL (3a), TiCrN–TiCrCN+TiBC ML (3b), and uncoated Pyrowear 675 (3c) in sliding contact with a Si₃N₄ indenter. (Pin-on-disk COF test data: WPAFB AFRL).

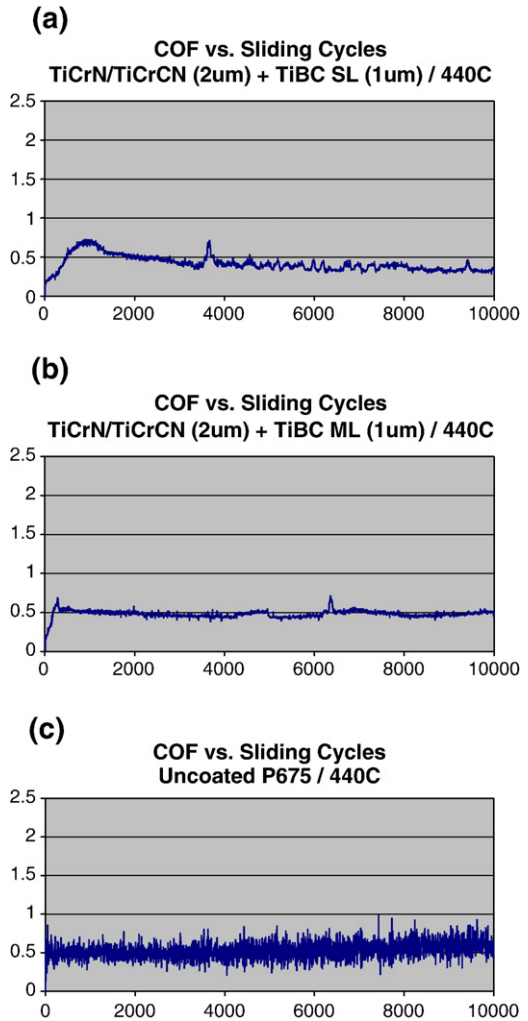


Fig. 4. Time dependant friction behavior of TiCrN–TiCrCN+TiBC SL (4a), TiCrN–TiCrCN+TiBC ML (4b), and uncoated Pyrowear 675 (4c) in sliding contact with a 440C indenter. (Pin-on-disk COF test data: WPAFB AFRL).

maximum friction values reached on 440C and Si₃N₄ for each coating: 0.45 for TiBC SL, and 0.75 for TiBC ML. In contrast to coated coupons, uncoated coupons either exhibited no time dependent behavior (uncoated vs. 440C, Fig. 4(c)), or erratic behavior that could not be characterized, as shown in Fig. 3(c) for an uncoated/Si₃N₄ pair. The steady state COF results in Figs. 3 and 4 demonstrate an improvement in friction behavior in contact with both 440C and Si₃N₄ for both TiBC SL and ML coatings over the uncoated condition in terms of predictable steady state frictional behavior, also indicating a steady and more predictable wear process. It was also observed that the steady state friction behavior was more stable for both TiBC SL and ML coatings in contact with Si₃N₄, where as friction data in contact with 440C showed a wider variation about the steady mean friction value.

3.2. Lubricated sliding wear testing results

Uncoated carbuzized Pyrowear 675, subjected to lubricated friction wear tests demonstrated a dominant abrasion wear mechanism resulting in severe mechanical damage. A profilometry

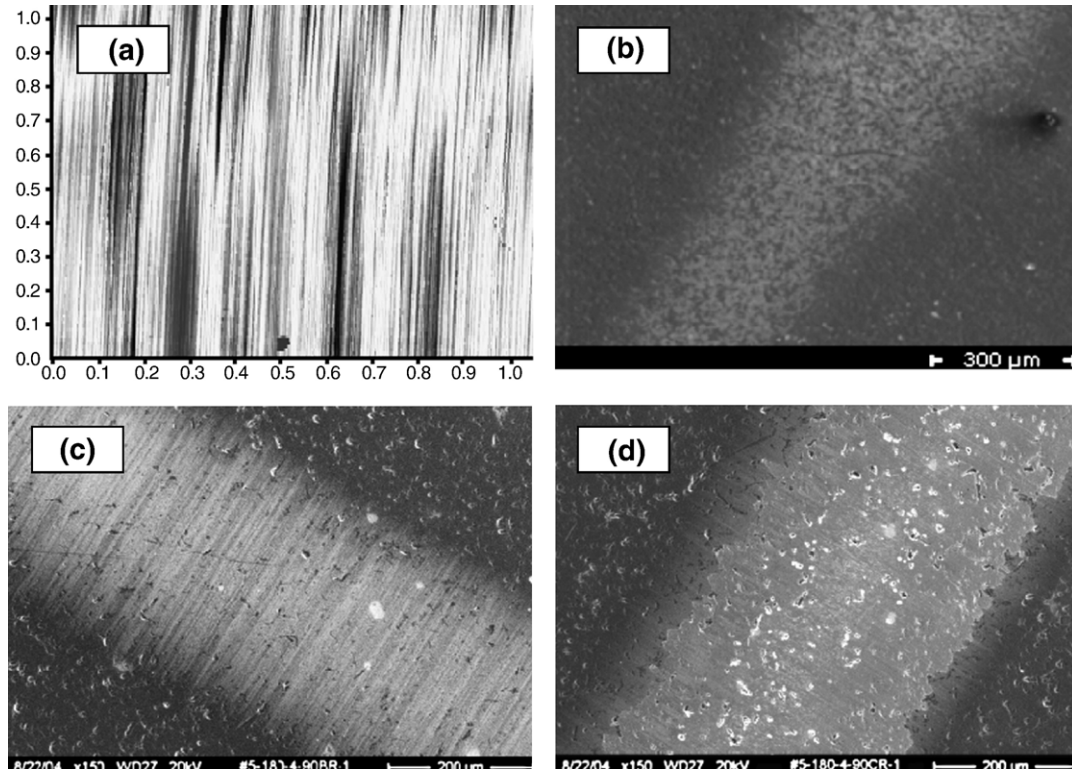


Fig. 5. Selected images of coupons subjected to lubricated sliding testing. (a) Coupon: uncoated P67, ring: uncoated Timken A4138 (linear scale is in mm). (b) Coupon: TiCrN/TiCrCN+TiBC SL, ring: uncoated Timken A4138. (c) Coupon: TiCrN/TiCrCN+TiBC ML, ring: uncoated Timken A4138. (d) Coupon: TiCrN/TiCrCN+TiBC ML, ring: 2.0 μm TiCrN/TiCrCN (Timken A4138).

scan of an uncoated P675 wear scar and SEM images of wear scars on coated carburized Pyrowear 675 are shown in Fig. 5(a–d). Fig. 5a shows a typical severe abrasive wear scar that was produced on an uncoated Pyrowear coupon in contact with an uncoated ring, adhesive material transfer to the ring was also observed. Polishing wear was found to be the primary mechanism for TiCrN/TiCrCN+TiBC SL coatings in contact with uncoated rings, Fig. 5b. Coated TiCrN/TiCrCN+TiBC ML samples in contact with uncoated P675 rings exhibited mild abrasion mechanisms, Fig. 5(c). Lubricated sliding testing using TiCrN/TiCrCN coated rings in contact with coated coupons showed more wear than with uncoated rings, and uncoated Pyrowear coupons in contact with

TiCrN/TiCrCN rings showed severe mechanical wear (Fig. 6). TiCrN/TiCrCN+TiBC SL coatings in contact with TiCrN/TiCrCN coated rings showed more abrasive wear than with uncoated rings, and TiCrN/TiCrCN+TiBC ML coatings demonstrated mixed adhesive/abrasive wear, Fig. 5(d). Posttest EDS composition mapping demonstrated that for coated samples, the coating was not completely removed from the surface after the test. Scanning profilometry images of the wear tracks caused by TiCrN/TiCrCN coated rings demonstrated improved wear resistance with TiCrN/TiCrCN+TiBC SL coatings (Fig. 6). Both TiBC SL and ML coating architectures performed well in lubricated sliding tests; TiBC SL demonstrated the best wear performance in contact with

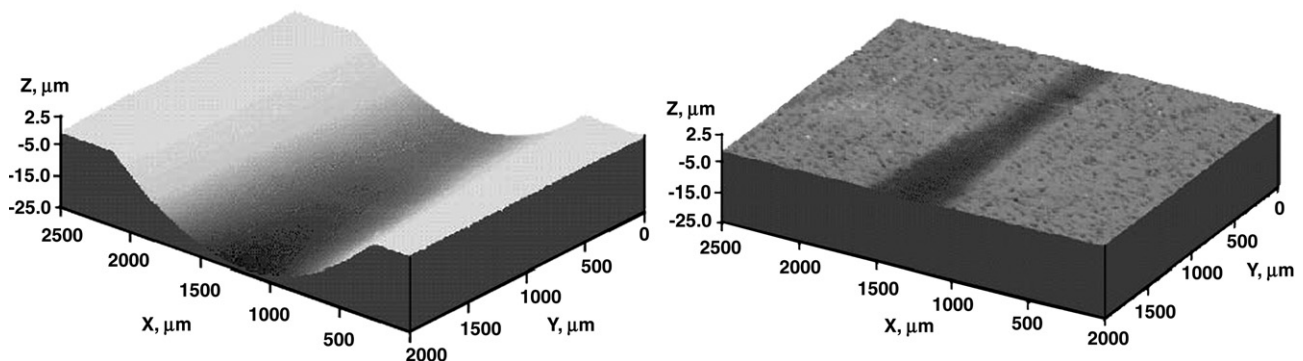


Fig. 6. Scanning profilometry image of lubricated sliding wear track, using a 2.0 μm TiCrN/TiCrCN coated ring on an uncoated carburized Pyrowear 675 coupon (left) and on a TiCrN/TiCrCN+TiBC SL coupon. Both scans are scaled to the same size for ease of relative comparison.

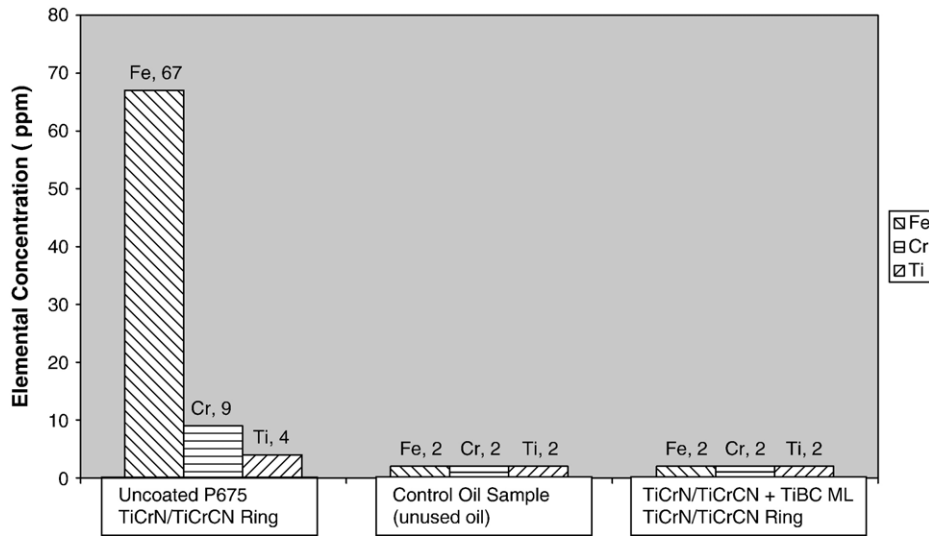


Fig. 7. Oil wear particle concentration results by ICP-MS for Fe, Cr, and Ti for coated 2.0 μm TiCrN/TiCrCN rings in contact with uncoated and coated coupons. Unused oil was also tested as a control; concentrations are recorded for the control due to the ICP-MS detection limit of 2 ppm.

uncoated rings, while the TiBC ML coating demonstrated the best wear performance in contact with TiCrN/TiCrCN coated rings. Testing results were further verified by induction coupled plasma mass spectrometry (ICP-MS) chemical analysis of oil used and collected during testing. Detection limits for the ICP-MS technique were Fe: 2 ppm, Cr: 2 ppm, and Ti: 2 ppm. Oil analysis results for TiCrN/TiCrCN coated ring lubricated sliding configurations tested by ICP-MS are shown in Fig. 7. Mild wear mechanisms observed in TiCrN/TiCrCN + TiBC ML sliding pairs were further supported by the ICP-MS data, which showed that Fe, Cr, and Ti wear particles were all below the detection limit. Large concentrations of Fe and Cr were observed in ICP-MS data supporting the observed severe abrasive wear for uncoated P675 coupons in contact with TiCrN/TiCrCN rings, Ti particles were also found indicating that some wear was occurring on the coated ring as well.

3.3. Reciprocating sliding testing results

Sharp coated scalers in non-lubricated reciprocating sliding contact with coated and uncoated coupons demonstrated wear mechanisms similar to lubricated sliding results. Uncoated carburized P675 coupons in contact with coated scalers exhibited abrasive wear mechanisms, while coated/coated pairs exhibited polishing wear. Typical testing results for dry reciprocating sliding are shown in Fig. 8. Fig. 8(a) shows the abrasive mechanism for uncoated coupons evident by wear grooves in the direction of sliding motion, in addition to abrasive wear, the contact surface also appeared to be covered with highly deformed wear particles indicating a plastic deformation wear mechanism as well. In contrast to the wear demonstrated by uncoated samples, coated samples demonstrated mild polishing wear, characterized by a minor reduction in surface roughness, but still maintaining the as deposited coating morphology, Fig. 8 (b). Coated scalers used in testing were not completely rigid and demonstrated an amount of flex during the reciprocating motion as a function of the contact friction force specific to the testing material pair. As a result, sliding pairs undergoing a greater

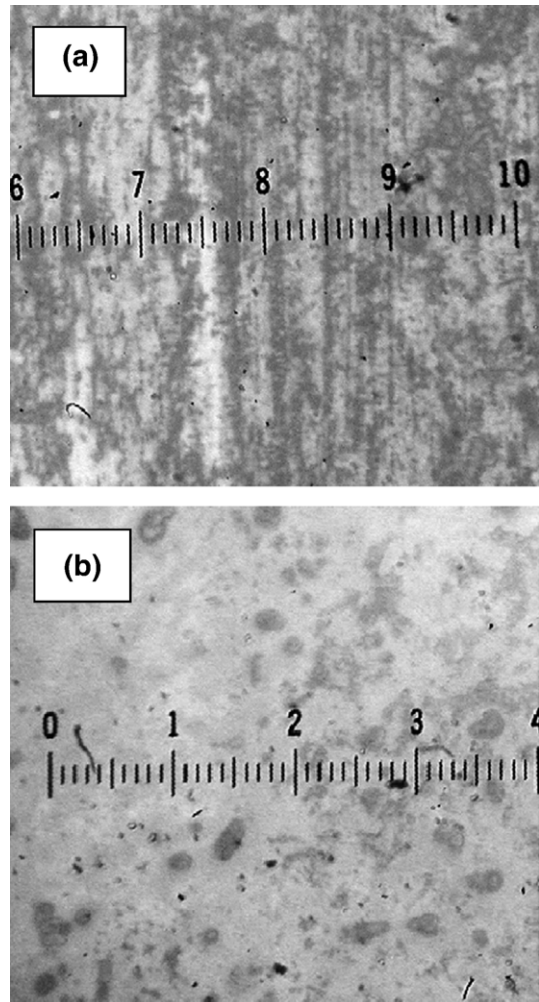


Fig. 8. Optical microscopy (1 major division = 52 μm) images of reciprocating dry sliding wear scars produced by a 440C scaler coated with 2.0 μm TiCrN/TiCrCN on (a) uncoated carburized P675 and (b) TiCrN/TiCrCN + TiBC ML coatings.

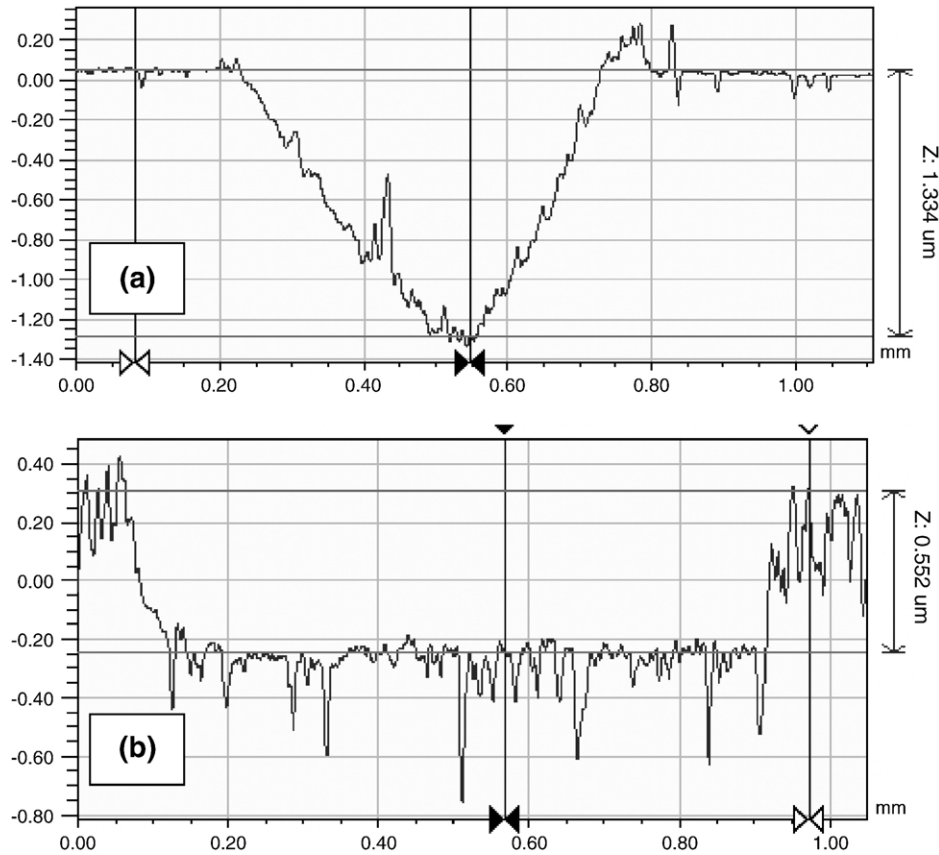


Fig. 9. Scanning profilometry 2D scans of dry reciprocating sliding wear scars produced by a 440C scaler coated with TiCrN on (a) uncoated carburized P675, damage step height 1.3 μm , and (b) TiCrN/TiCrCN+TiBC ML, damage step height 0.55 μm .

friction wear process developed shorter wear scars due to scaler flex. Linear micrometry was used to characterize the relative friction between sliding pairs with lubricated reciprocating sliding acting as a baseline with a consistent wear scar length of 740 μm for both uncoated and coated pairs. Wear track lengths for uncoated carburized P675 in dry sliding contact with coated scalars were consistently shorter at $\sim 570 \mu\text{m}$, indicating a relatively high friction wear process. TiCrN/TiCrCN+TiBC (SL and ML) coatings in dry sliding contact with coated scalars produced consistent wear scars of $\sim 740 \mu\text{m}$, indicating that the friction in dry sliding was comparable to the boundary lubrication friction in lubricated reciprocating sliding. Mechan-

ical wear of uncoated Pyrowear 675 in dry sliding against a coated scalar was characterized primarily by single body wear of the uncoated coupon resulting in relatively deep, 1.25 μm –1.5 μm , narrow wear scars (Fig. 9(a)), and minor polishing wear developed on the coated scaler. Coated dry sliding pairs were characterized by two body polishing wear as indicated by the relatively wide wear scars on the coupon flat (Fig. 9(b)) formed by a mutually worn scaler, and wear depths of 0.45 μm –0.6 μm . Lubricated reciprocating sliding testing showed effective boundary lubrication with minimal asperity contact under the given testing conditions, resulting in negligible damage to coated and uncoated coupons.

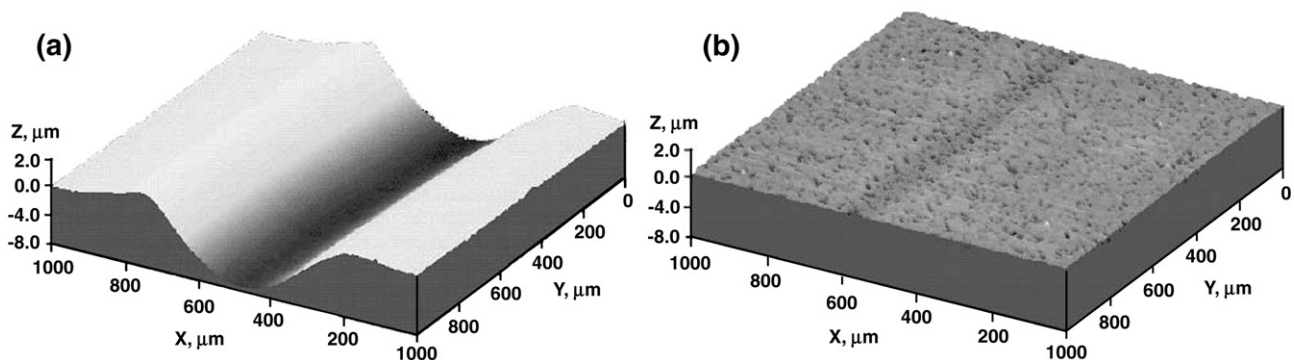


Fig. 10. Scanning profilometry wear track images of 3.2 GPa rolling contact /hot PFPFAE-based lubricant testing of (a) uncoated and (b) TiCrN/TiCrCN+TiBC ML coated P675.

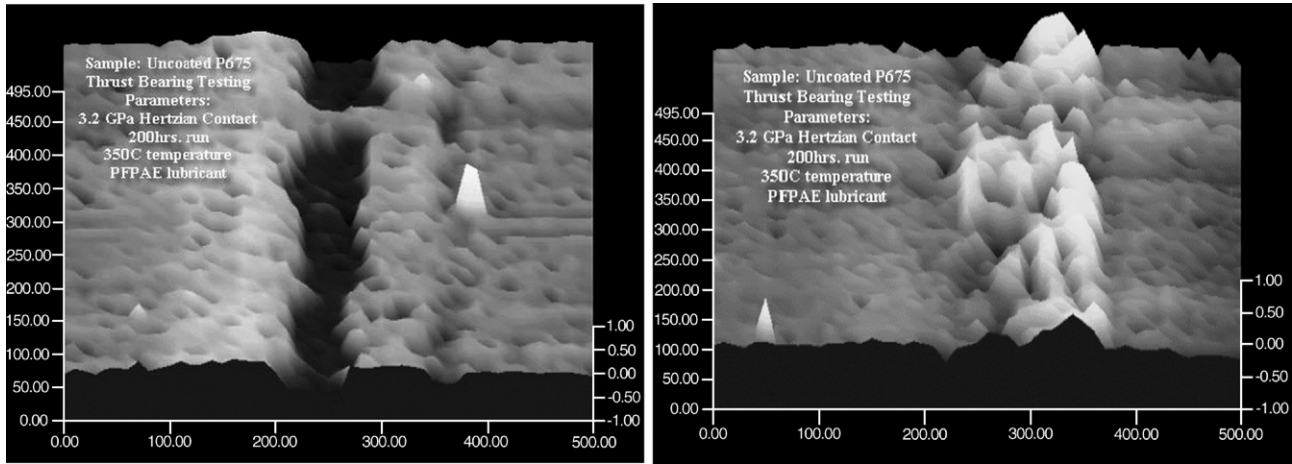


Fig. 11. Scanning profilometry wear track images of 3.2 GPa rolling contact/350 °C PFPAAE-based lubricant testing conducted on uncoated P675 for 23 h. (left), and 200 h. (right). Corrosion products (primarily iron oxide) completely filled the 200 h. Wear track, forming an ~0.2 μm step height elevated surface.

3.4. High load rolling contact/high temperature PFAPE lubricant compatibility testing results

Results for hot PFPAAE corrosion under high load rolling conditions established dramatic differences between TiBC coating configurations and uncoated Pyrowear 675 samples. Initial tests were conducted for 2 h at standard test conditions with repeated results as shown in Fig. 10. Testing durations of 2 h demonstrated relatively large, 4–8 μm deep, plastic wear track deformations occurring in the uncoated sample in comparison to the coated samples, which showed only minor deformation in the form of a local reduction in the coating surface roughness. SEM analysis of 2 h test durations for coated and uncoated samples showed minimal chemical interaction, including possible initiations of oxidation observed as discolored areas with uncoated samples, and mild discoloration with coated samples. Extended testing of uncoated Pyrowear samples, for 23 h, and 200 h, identified an aggressive corrosion process not seen in 2 h test runs, scanning profilometry results are shown in Fig. 11. Scanning profilometry results from 2–200 h uncoated Pyrowear testing suggests that the wear track

formation process is initially dominated by mechanical deformation, followed by a corrosion process, which, over time, fills the wear track and forms a new, elevated track surface. Observation that the corrosion process is localized on the wear track would also suggest that the corrosion process is affected by contact pressure. Test results for 20–200 h TiCrN/TiCrCN+TiBC SL and TiCrN/TiCrCN+TiBC ML were very similar, for simplicity, only results for the TiCrN–TiCN+TiBC ML coating are presented. TiCrN–TiCN+TiBC ML samples demonstrated very different wear track characteristics in comparison with uncoated samples, as shown in Fig. 12. Scanning profilometry results for 23 h TiCrN/TiCrCN+TiBC ML coated test samples showed minimal wear track damage. For 2 out of 3 samples only reductions in the surface coating roughness were detectable. One 23 h coated sample (Fig. 12 (left)) showed considerable wear track formation in the location measured, with a track width of ~0.5 μm, a step depth of ~1.0 μm, and a similar 2-D profile to those produced in the 23 h uncoated sample. Wear track results for the 200 h coated sample test were characteristic of a mechanically dominated process involving plastic deformation of the substrate rather than a

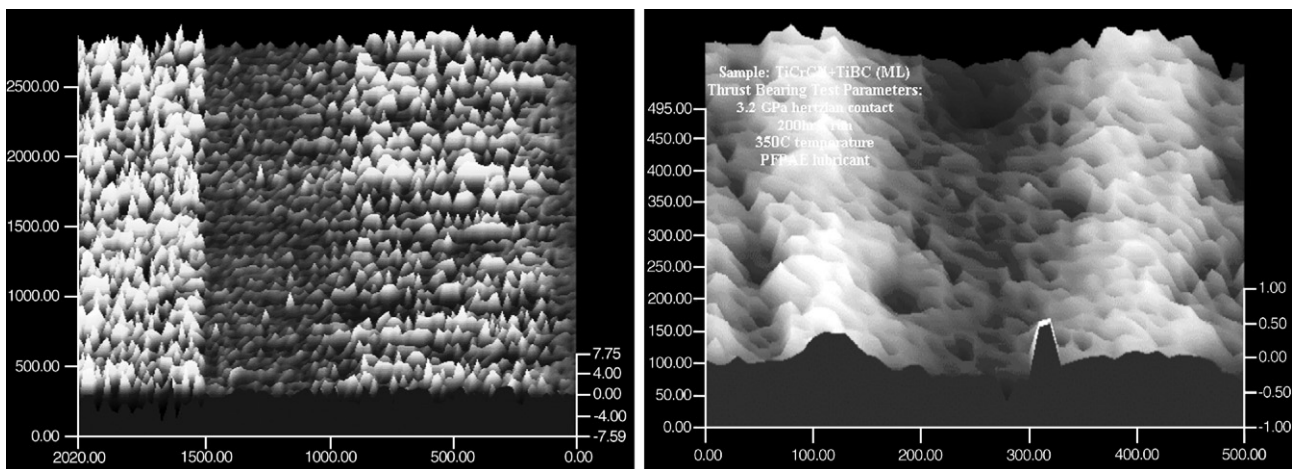


Fig. 12. Scanning profilometry wear track images of 3.2 GPa rolling contact/350 °C PFPAAE-based lubricant testing conducted on TiCrN/TiCrCN+TiBC ML for 23 h. (left), and 200 h. (right).

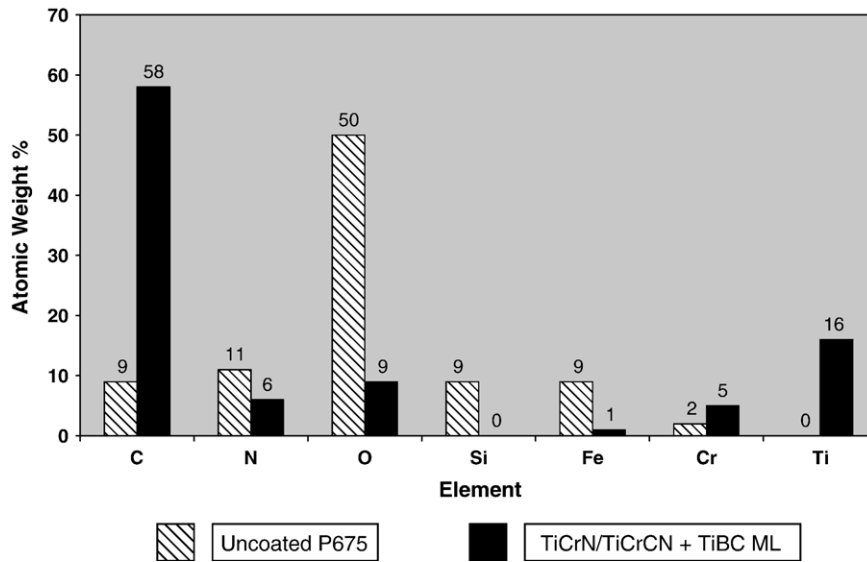


Fig. 13. Surface chemistry by EDX of high load, high temp PFPAE lubricant testing wear tracks for an uncoated P675 sample and TiCrN/TiCrCN+TiBC ML samples after 200 h testing.

corrosion process (Fig. 12(right)). Wear track 2-D profiles showed deformation conformal to the ball bearing indenter with a step depth of 0.25 μm . Visual, SEM, and EDX surface analysis was conducted to determine the high temperature PFPAE lubricant compatibility of TiCrN/TiCrCN+TiBC ML coated samples in comparison to uncoated carburized P675 samples, with specific consideration given to the aggressive corrosion process observed visually and by profilometry in uncoated sample wear tracks. EDX analysis for an uncoated sample tested for 23 h showed an increase in nitrogen surface content within the wear track (Fig. 11(left)), possibly indicating film formation from the breakdown of the Krytox lubricant. Sections of the film within the wear track appeared to be subject to spallation, uncovering areas with compositions similar to baseline P675 EDX measurements. No significant increases in wear track oxygen content were measured indicating oxidation mechanisms were not dominant by 23 h of testing. Further EDX analysis of 23 h uncoated wear tracks (Fig. 11(left)) showed multiple sites of $\sim 4 \mu\text{m}^2$ silicon inclusions, and EDX of Si_3N_4 balls showed significant ($\sim 12\%$ atomic weight) iron particle transfer to the testing ball surface and a slight ($\sim 4\%$ atomic weight) increase in ball surface oxygen content, indicating that some wear was occurring of the Si_3N_4 balls, but initial chemical/mechanical wear primarily resulted in the formation of oxidized iron particles. The results found by surface profilometry for wear tracks formed after 200 h of testing for the uncoated and coated samples were re-iterated by EDX analysis (Fig. 13). EDX results shown in Fig. 13 show a $\sim 50\%$ atomic weight measured for oxygen in the uncoated wear track (Fig. 11(right)) as compared to a $\sim 9\%$ atomic weight measured for oxygen in the coated wear track (Fig. 12(right)), demonstrating the excellent corrosion/oxidation resistance of the TiCrN/TiCrCN+TiBC ML (and SL) coating configuration in the presence of PFPAE based solid lubricants at high temperature. Silicon content in the wear track was measured at

$\sim 9\%$ atomic weight, while no silicon was recorded in the coated sample wear track. EDX analysis of Si_3N_4 balls used in testing showed an increase in the iron transfer layer over 23 h results at $\sim 12\%$ atomic weight to $\sim 20\%$ atomic weight in contact with uncoated coupons tested for 200 h. No iron was found on the surface of ball for 200 h testing in contact with the

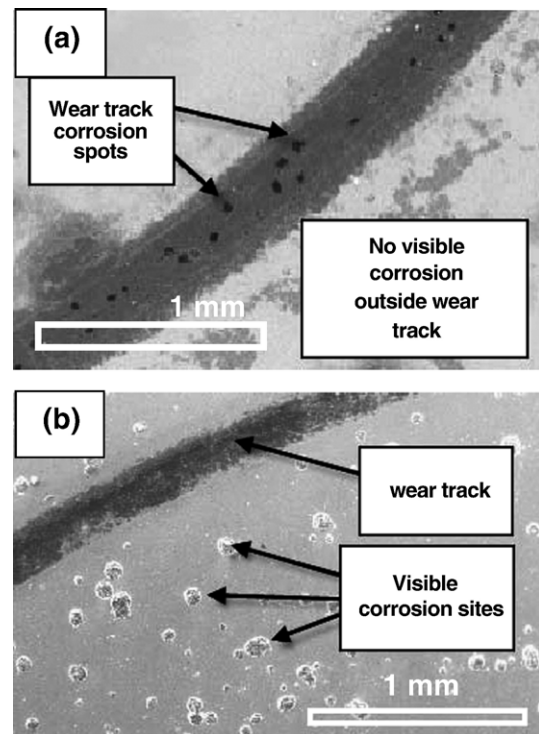


Fig. 14. (a) TiCrN/TiCrCN+TiBC ML coating wear track/surface after 200 h 3.2 GPa 350 $^\circ\text{C}$ rolling contact PFPAE lubricant compatibility testing. (b) Uncoated carburized P675 wear track/surface after 200 h 3.2 GPa 350 $^\circ\text{C}$ rolling contact PFPAE lubricant compatibility testing.

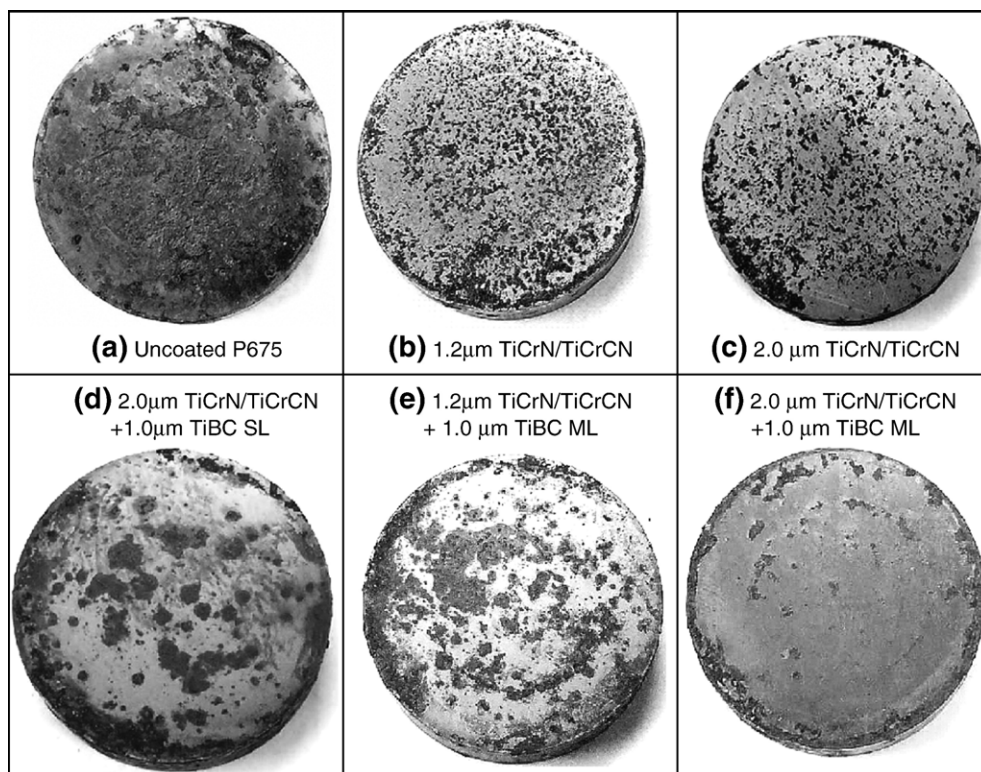


Fig. 15. (a–f) Selected images of test coupons after MIL-STD-810F “salt-fog” testing.

coated coupon. Dark areas within the wear track for the coated sample were observed (Fig. 14(a)) and found to be nitrogen rich by EDX, possibly indicating that the TiCrN/TiCrN segment was exposed and isolated areas of wear track corrosion may have penetrated the top TiBC ML segment. However, the bottom segment coating was assumed to be intact since EDX analysis did not measure any iron content within the penetrated areas. For the 200 h uncoated sample multiple large iron oxides (~50 at.% oxygen by EDX) sites were observed visually and by SEM on the sample surface (Fig. 14(b)). Corrosion sites outside of the wear track were not optically visible for the coated sample (Fig. 14(a)), however corrosion sites were discovered by SEM at areas where the substrate and hence the coating was flawed (surface scratches) prior to coating deposition and testing.

3.5. Corrosion testing results

Results for MIL-STD-810F “salt fog” corrosion testing of uncoated and coated carburized P675 are presented in Fig. 15(a–f). Corrosion testing results for the uncoated carburized Pyrowear 675, Fig. 15(a), showed the widespread formation of iron and chromium oxide scale resulting in a dramatic increase in surface roughness. Severe oxidation and pitting corrosion were identified along with evidence of extensive oxide scale spallation. Corrosion results for the coated coupons showed marked improvement in corrosion resistance over uncoated carburized P675. All coated samples developed more severe corrosion around the coupon edges (poor coating adhesion area), or areas surrounding the circular wear track produced by prior

thrust bearing testing (damaged areas). Corrosion testing was conducted for partial architectures, Fig. 15(b)–(c), to determine the effect of the bottom segment TiCrN–TiCrCN coating thickness on corrosion resistance. TiCrN/TiCrCN coating configurations, Fig. 15(b)–(c), demonstrated a slight improvement in corrosion resistance by increasing the coating thickness from 1.2 µm to 2.0 µm. Pitting corrosion was the primary mechanism for TiCrN/TiCrCN samples, characterized by pure metallic dissolution with little or no oxide formation. Corrosion resistance results were more improved for an increase in bottom segment thickness with the top coating segment included, Fig. 15(d)–(f). The 2.0 µm TiCrN/TiCrCN+1.0 µm TiBC ML coating configuration demonstrated a marked improvement over the 1.2 µm TiCrN/TiCrCN+1.0 µm TiBC ML thick counterpart Fig. 15(e), developing pitting/oxide corrosion primarily in “damaged” (coupon edges, near wear track) areas only. The 2.0 µm TiCrN/TiCrCN+1.0 µm TiBC SL architecture did not perform as well as the comparable ML coating, Fig. 15(d), performance of the thick TiBC SL architecture was characterized by pitting and oxide formation were similar to the thin 1.2 µm TiCrN/TiCrCN+1.0 µm TiBC ML variant.

4. Conclusion

Nano-structured coating architectures were developed to provide a best blend of corrosion and wear resistance for high chromium content steels used in aerospace bearing and gear applications. Testing results for the friction, wear, and corrosion behaviors of the multi-segment TiCrN/TiCrCN+TiBC coating

system applied to carburized Pyrowear 675 substrates showed marked improvements in corrosion resistance and wear properties when compared to uncoated Pyrowear 675. From the results of this study a number of general conclusions were drawn:

- (1) Coated samples demonstrated reductions in dry sliding friction by 1.3–2 times over uncoated samples. All coated samples demonstrated predictable time dependent friction behavior, translating to predictable wear.
- (2) TiCrN/TiCrCN+TiBC SL samples demonstrated less aggressive “run-in” friction in dry sliding COF testing, as compared to TiCrN/TiCrCN+TiC/TiBC (ML) which ramped to maximum friction values in $\sim 1/4$ of the sliding cycles of TiBC (SL) coatings.
- (3) High load lubricated sliding test results for uncoated P675 samples were characterized by severe mechanical wear with wear track depths on the order of 20 times those measured for coated samples.
- (4) Initial results show that TiCrN/TiCrCN+TiBC SL coatings perform better in lubricated sliding applications against uncoated Timken bearing steel, exhibiting mild two body polishing wear, than TiBC ML coatings, which exhibited mild abrasive wear. It is assumed that the TiBC ML top segment architecture, which is optimized to reduce crack tip energies for fatigue applications, may produce more wear particles which in turn further contribute to abrasion mechanisms in lubricated sliding contact due to sequential layer by layer delamination failure. In contrast, for contact with TiCrN/TiCrCN coated rings the TiCrN/TiCrCN ML coating performed better than the TiCrN/TiCrCN SL coating.
- (5) TiCrN/TiCrCN+TiBC (SL and ML) coatings demonstrated excellent performance in high load, high temperature, rolling contact PFPPE lubricant compatibility testing. Coated coupons demonstrated minor mechanical wear track deformations, no material transfer to testing balls, no visible corrosion sites outside of the wear track, and minor wear track corrosion sites after 200 h of testing that did not penetrate the bottom coating segment. Uncoated coupons developed mechanical deformed wear tracks within 2 h of testing on the order of 4–8 times the depth of coated coupons, along with material transfer to the testing balls. Wear tracks for uncoated coupons were completely filled in with corrosion after 200 h of testing, and multiple corrosion sites were visible outside of the wear track.
- (6) Corrosion testing showed that increasing TiCrN/TiCrCN bottom segment thickness from 1.2 μm to 2 μm has a positive effect on corrosion resistance, and further increase in thickness would be expected to produce further improvement in corrosion performance. Coupons tested with the top segment included also showed improved corrosion resistance, with the best performance exhibited by the TiBC ML coating. All coated coupons showed an improvement in corrosion resistance over uncoated Pyrowear 675.

Acknowledgements

The authors would like to acknowledge the technical assistance of Recep Avci and Jim Anderson at Montana State University. Thanks to Duane Jones for carrying out some of the coating deposition trials. Thanks are also due to Bob Horowitz and Al Deckmar for help in sample fixture preparation and initial corrosion resistance testing. Portions of this research were supported by the United States Department of Defense via the Small Business Innovation Research (SBIR) Program, and managed by AFRL, Wright Patterson AFB Materials and Manufacturing Directorate.

References

- [1] N. Novikov, V.I. Gorokhovskiy, B. Uryukov, Surf. Coat. Technol. 47 (770) (1991).
- [2] Vladimir Gorokhovskiy, Brad Heckerman, Philip Watson, Nicholas Bekesch, Surf. Coat. Technol. 200 (18–19) (2006) 5614.
- [3] E. Bertran, C. Corbella, A. Pinyol, M. Vives, J.L. Andujar, Diamond Relat. Mater. 12 (2003) 1008.
- [4] E. Martinez, U. Wiklund, J. Esteve, F. Montala, L.L. Carreras, Wear 253 (2002) 1182.
- [5] K. Bewilogua, C.V. Cooper, C. Specht, J. Schroder, R. Wittorf, M. Grischke, Surf. Coat. Technol. 132 (2000) 275.
- [6] Philip C. Yashar, William D. Sproul, Vacuum 55 (1999) 179.
- [7] Roland Hauert, Jorg Patscheider, Adv. Eng. Mater. 2 (5) (2000).
- [8] A.A. Voevodin, S.D. Walck, J.S. Zabinski, Wear 203/204 (1997) 516.
- [9] A.A. Voevodin, J.S. Zabinski, C. Muratore, Tsinghua Sci. Technol. 10 (2005) 665.
- [10] M. Jonston, J. Laritz, M. Roads, Thin Dense Chrome Insertion Program Pyrowear 675 and Cronidar Wear Testing, Report No.R98AEB240, GE Aircraft Engines Advanced Engineering Program Department Cincinnati, OH.
- [11] Available http://www.carttech.com/products/wr_products_bearing_pyrowear.html.
- [12] Vladimir I. Gorokhovskiy, Rabi Bhattacharya, Deepak G. Bhat, Surf. Coat. Technol. 140 (2) (2001) 82.
- [13] Carvalho, N.J.M. Ph.D. Thesis Rijksuniversiteit Groningen, 2001 ISBN 90 367.
- [14] J.A. Jehn, Surf. Coat. Technol. 125 (2000) 212.
- [15] H.-S. Park, H. Kappl, K.H. Lee, J.-J. Lee, H.A. Jehn, M. Fenker, Surf. Coat. Technol. 134–134 (2000) 176.
- [16] M. Jarratt, J. Stallard, N.M. Renevier, D.G. Teer, Diamond Relat. Mater. 12 (2003) 103.
- [17] D. Sanders, A. Anders, Surf. Coat. Technol. 139 (2000).
- [18] In-Wook Park, Kwang Ho Kim, A.O. Kunrath, D. Zhong, J.J. Moore, A.A. Voevodin, E.A. Levashov, J. Vac. Sci. Technol., B 23 (2005) 588.
- [19] A.A. Voevodin, J.S. Zabinski, in: A.A. Voevodin, D.V. Shtansky, E.A. Levashov, J.J. Moore (Eds.), Nanostructured Thin Films and Nanodispersion Strengthened Coatings, Kluwer Academic Publishers, Dordrecht, The Netherlands, 2004, p. 103.
- [20] P.S. Kisliiy, M.A. Kusenikova, N.I. Bodnaruk, B.L. Grabchuk, Boron Carbide, Naukova Dumka, Kiev, 1988 in Russian.
- [21] V. Gorokhovskiy, C. Bowman, P. Gannon, D. VanVorous, A.A. Voevodin, A. Rutkowski, C. Muratore, R.J. Smith, A. Kayani, D. Gelles, V. Shutthanandan, B.G. Trusov, Tribological performance of hybrid filtered arc-magnetron coatings. Part I: Coating deposition process and basic coating properties characterization, Surf. Coat. Technol. 201 (6) (2006) 3732.
- [22] Anthony C. Fisher-Cripps, Introduction to Contact Mechanics, 1st edition, Springer, 2000.
- [23] ASTM B117-03 “Standard Practice for Operating Salt Spray (Fog) Apparatus”, ASTM International.